Neutronics Simulations for the Design of Neutron Flux Monitors in SPARC

X. Wang[1*], R. Gocht[2], J. Ball[1], S. Mackie[1], E. Panontin[1], R.A. Tinguely[1],
P. Raj[2], I. Holmes[2], A.A. Saltos[2], A. Johnson[2], A. Grieve[2]

[1]*Plasma Science and Fusion Center, MIT, Cambridge, MA 02139*
[2]*Commonwealth Fusion System, Devens, MA 01434*
** The author to whom correspondence may be addressed: wxinyan@mit.edu*

ABSTRACT
This paper presents the development and application of high-fidelity neutronic models of the SPARC tokamak for the design of neutron flux monitors (NFM) during plasma operations. NFMs measure the neutron flux in the tokamak hall which is related to fusion power via calibration. We have explored Boron-10 gamma-compensated ionization chambers (IC) and parallel-plate Uranium-238 fission chambers (FC). We plan for all NFMs to be located by the wall in the tokamak hall and directly exposed to neutrons streaming through a shielded opening in a midplane port. This project primarily uses a constructive solid geometry (CSG)-based OpenMC model based on the true SPARC geometry. The OpenMC model is benchmarked against a CAD-based MCNP6 model. The B10 ICs are equipped with high-density polyethylene (HDPE) sleeves, borated HDPE housings, and borated Aluminum covers to shield out scattered neutrons, optimize detector response levels, and make calibration robust against changes in the tokamak hall. The B10 neutron absorption branching ratio can be a potential issue for >200 keV neutrons. However, our simulations unveil that, in the SPARC environment and with the proposed housings and sleeves, > 99% of B10 NFM signals are induced by < 100 keV neutrons. U238's insensitivity to slow neutrons makes this FC a promising candidate for direct fusion neutron measurements. Along with a borated HDPE sleeve to further prioritize direct neutrons, about 60% of the FCs' responses are induced by direct neutrons.

I. INTRODUCTION

Fusion neutrons, as products of DT fusion reactions, carry information about the fusion plasma, including fusion power, ion temperatures, neutron emissivity profiles, etc. Thanks to neutrons' long mean free paths, these parameters can be obtained by measuring neutrons outside the tokamak and away from the harsh plasma environment. Neutron flux monitors (NFM) are one of the neutron diagnostic systems planned for SPARC. They measure the local neutron flux in the tokamak hall and convert the measurement to fusion power through calibrations. This paper introduces the OpenMC[1] neutronics modeling work for the design of NFMs for the SPARC[2] tokamak by Commonwealth Fusion Systems (CFS). This paper focuses on two options: B10-coated ionization chambers (IC) and U238 fission chambers (FC). Additional flux-shaping parts are applied to optimize signal strength, direct/total neutron ratio, robustness of calibrations to changes in the tokamak hall, and flat response, which means DT and DD plasma emitting neutrons at the same rates, despite different energies, should induce the same responses to certain NFMs. B10 ICs and U238 FCs combined are proposed to cover the entire plasma operation range, and more NFMs for the calibration range are under investigation. Calibration neutron sources such as neutron generators and radioactive isotopes are much less powerful than the plasma source during operation, so these calibration-range NFMs must be of a type that has higher sensitivity, such as proportional counters[3].

The implementation and verification of the OpenMC SPARC model will be covered in Section II. Section III will introduce the design and modeling work for the B10 ICs and U238 FCs. The potential effects of B10's branching ratio in a fast neutron environment will also be discussed. Conclusions and future work on SPARC NFMs will be summarized in Section IV.

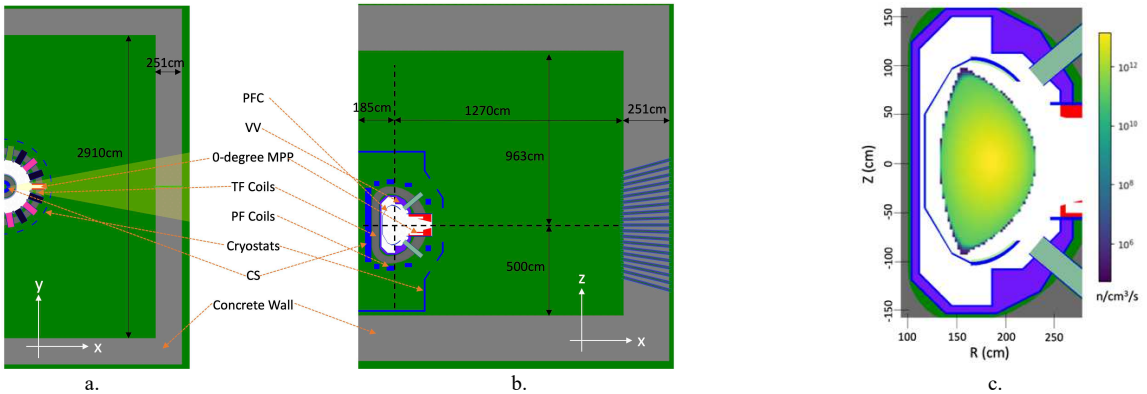

a. b. c.

Figure 1. OpenMC SPARC Model. a. XY View (+X Half). b. XZ View (+X Half). c. Neutron Emissivity from TRANSP Kinetic Profiles. Dark Grey: TF Coils. Purple: VV. Red: 0MPP. Blue: Stainless Steel Parts, including CS, PF Coils and the Cryostat. Dark Green: Air. Light Grey: Concrete Tokamak Hall Wall. On the +X wall are 19 collimators. See Section II.A for the full names of the acronyms.

II. OpenMC SPARC Model

A. Model Overview

The OpenMC model of SPARC is shown in Figure 1a and b. It features key components including plasma facing components (PFC), tokamak vacuum vessel (VV), toroidal field (TF) coils, poloidal field (PF) coils, central solenoid (CS), cryostat, and port shieldings. The PFC has a Tungsten layer and a stainless steel (SS, mainly Iron and Chromium) layer. The divertor and other PFCs are not explicitly modeled. The 0-degree midplane port (0MPP) with opened shielding for neutron diagnostics is modeled in more detail for higher fidelity. Other ports are modeled as homogenized blocks with material compositions preserved. The TF coils are modeled as a homogenized Boron Carbide (B4C) + SS case. The cryostat, PF coils, and CS are all modeled as SS. Figure 1c is the DT fusion neutron emissivity for SPARC's primary reference discharge (PRD)[3] calculated based on ion density and temperature profiles from the TRANSP code[4,5] and Bosch-Hale reactivities[6]. OpenMC treats this source as a 50x80 matrix of finite element rings of 14.1 MeV fixed sources thermal broadened by local ion temperature. Within each ring, the volumetric source intensity is uniform.

B. Verification

The OpenMC model is verified with a CAD-based MCNP6[7] model from CFS. Neutron spectra in a shell just outside the tokamak, i.e. in the tokamak hall, are compared. Both the models were run in 20-degree mode centered at 0 degrees with reflective side boundaries as shown by the shaded area in Figure 1a.

Results are shown in Figure 2. The OpenMC model generally agrees well with the CAD-based MCNP model, which proves the OpenMC model's reliability as a scoping tool. In the fast range, the OpenMC results are higher than the MCNP results by a factor of 3 because the 0-degree port shielding in MCNP is not as open as the one in OpenMC. The discrepancies in the thermal range might be due to the differences between the CSG-based and detailed CAD-based approaches. Thermal neutrons are less penetrating, so they are more likely to be affected by details in the geometry. However, thermal neutrons do not carry a lot of energy and especially have little effect on the neutron diagnostic system, which primarily focuses on fast neutrons.

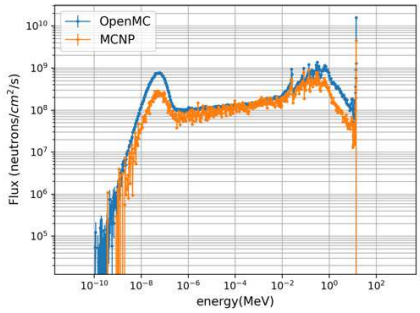

Figure 2. OpenMC vs MCNP in a Shell Outside of the Tokamak. Source Rate = 5E19 n/s.

The 20-degree model is only used for verification. All other simulations in this paper were done in 90-degree mode.

III. NEUTRON FLUX MONITORS

A. Neutrons in SPARC

A CAD-based MCNP-simulated fast neutron flux map is shown in Figure 3. The source rate is 5E19 n/s corresponding to SPARC's 140 MW PRD. Compared to thermal neutrons undergoing extensive, fast neutrons retain more information about the plasma, so NFMs will be placed in the bright red/orange region to measure as many fast neutrons as possible while maintaining ease of construction.

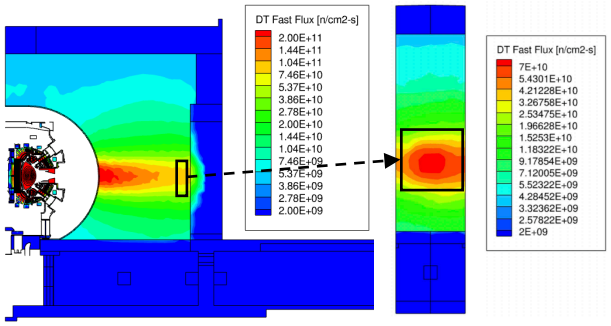

Figure 3. a. XZ View. b. YZ View by the Wall. Fast (> 1 MeV) Neutron Flux Map in SPARC Tokamak Hall. Uncertainties in the Tokamak Hall < 15%. Source Rate = 5E19 n/s.

The layout of the NFM fleet is shown in Figure 4. There are four B10 ICs, four U238 FCs, and more housings reserved for other NFMs. The central line of gray square tubes are collimators for neutron cameras[8] and a neutron spectrometer[9]. The rest of this section will discuss the neutronics aspect of the design of the flux-shaping materials for these NFMs.

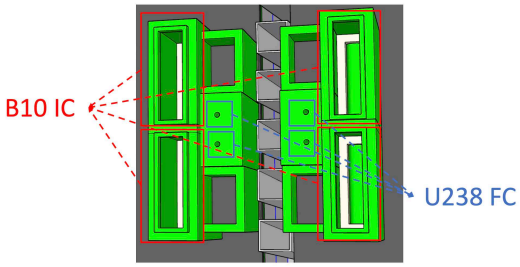

Figure 4. NFM Fleet Layout. Dark Grey: Concrete Wall. Light Grey: Collimators. Green: HDPE or B-HDPE.

Besides DT neutrons, 2.5 MeV DD neutrons are also a consideration for NFM designs: SPARC will have a dedicated DD commissioning campaign, and DD fusions are possible in DT plasma. As a result, B10 ICs shall have flat responses to DT and DD neutrons.

B. B10 Coated Gamma-Compensated Ionization Chamber

B10 ICs detect neutrons by measuring B10 neutron absorption reaction products, which means detector responses should be proportional to the absorption rates. B10 ICs have high sensitivities thanks to B10's high thermal neutron absorption cross sections[10]. There are many off-the-shelf options, some with gamma compensation capabilities. Gamma noises, including neutron-induced gamma, fusion

gamma, etc., are common in Tokamak, so such capability to cancel gamma signals in the detector is highly desirable.

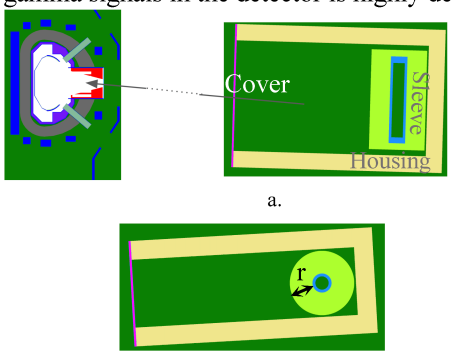

Figure 5. a. B10 IC Side View (XZ). b. B10 IC Top/Down View (XY). B10 IC and its Shielding. Yellow: B-HDPE Housing, Pink: B-Al Cover. Light Green: HDPE Sleeve. Light Blue: Aluminum Case of the IC Unit. The Arrow Indicates the Direction the Housing is Facing.

The proposed design of B10 IC is shown in Figure 5. Since B10 ICs are intrinsically sensitive to thermal neutrons while DT fusion neutrons are 14.1 MeV, a High-Density Polyethylene (HDPE) cylindrical sleeve is added to locally moderate fast neutrons. Also, to filter out scattered neutrons from the surroundings so as to prioritize direct neutrons from the plasma, a Borated-HDPE (B-HDPE) housing with an opening facing toward the 0MPP is added. The housings are also expected to make calibration robust against changes in the tokamak hall, which can affect scattered neutrons and thus potentially NFM responses. The performance is under scoping. Finally, to cut off thermal neutrons from the front, a thin borated aluminum (B-Al) cover is added.

1. *Housing*

The housing wall thickness will be 5-10 cm. The final decision shall balance neutron shielding performance and volumes. Figure 5 compares neutron spectra around the IC units with and without the housing. The housing cuts ~80% < 0.1 eV neutrons, ~50% < 0.1 MeV neutrons, and has little effect on the 14 MeV peak, which fulfills its goals well.

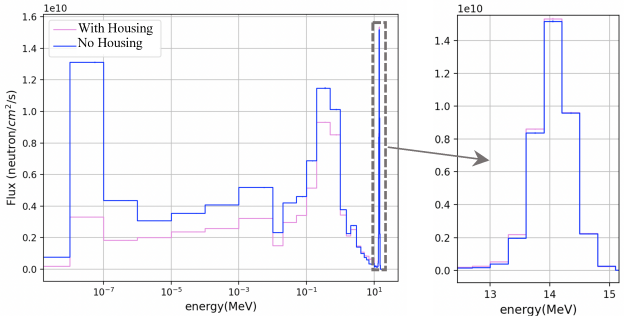

Figure 6. Neutron Flux around the ICs with vs. without the Housing. Housing Thickness = 5 cm. IC Sleeve Thickness = 6 cm. No B-Al Cover. Source Rate = 5E19 n/s.

2. *Borated Aluminum Cover*

The cover has a sandwich structure with 0.5 mm aluminum on both sides and 5 mm borated aluminum in the middle. To examine the effects of the cover, we tallied the neutron spectra inside the housings but outside of the sleeves. Results with 20% B4C + 80% Aluminum cover, 40% B4C + 60% Aluminum cover, and no cover are plotted in Figure 7 and the relative differences are in Figure 8. The cover effectively reduces < 1 eV neutrons (20% - 40% reduction), but cannot remove all of them since some are produced within the housing. The cover also slightly reduces higher-energy neutrons. In the 11-13 MeV range, cases with B-Al covers have slightly higher neutron flux. This could be due to that 14 MeV neutrons are scattered into the [11, 13] MeV range by the Aluminum. The close performance of the 20% B4C and 40% B4C cover indicate that 20% already cuts most of the thermal neutrons from the front and is enough for its purposes.

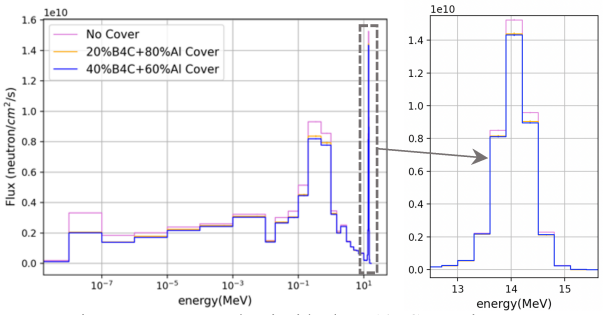

Figure 7. Neutron Flux inside the B10 IC Housings. Sleeve Thickness=6cm. Source Rate = 5E19 n/s.

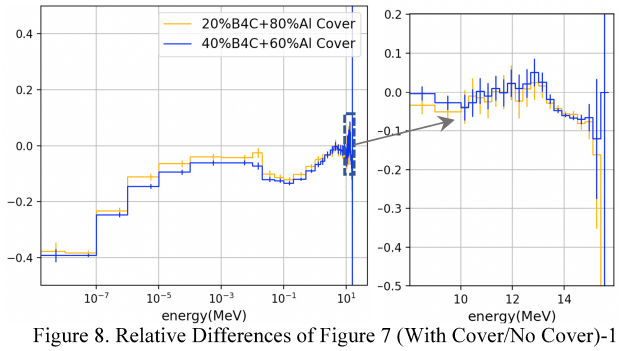

Figure 8. Relative Differences of Figure 7 (With Cover/No Cover)-1.

3. *HDPE Sleeves*

Reasonably thick HDPE sleeves can better moderate fast neutrons and thus improve the B10 IC's signals, but overly thick sleeves can block neutrons and reduce the signals. To quantify this effect, simulations were launched to compute the detector response as a function of sleeve thickness (r in Figure 5b). The 40% B-Al cover is used for this scoping. The results are summarized in Figure 9. Note that 1) only the side thickness of the sleeve is varying while top/bottom thickness stays at 2 cm, and 2) the inner width of the housing is changing to fit the sleeves while minimizing the width to better filter out thermal neutrons. The larger the housing openings are, the wider the fields of view (FOV) are, and the NFMs are seeing more regions other than the opening port. These regions are sources of scattered neutrons. Thus, the housing openings should be as small as possible. As

predicted, the detector response increases with increasing sleeve thickness for small sleeve thicknesses because of better moderation but then decreases because of blocking effects. 7 cm is the best for signal strength, while 12 cm provides a flat response. The 7 cm sleeve's detector response to DD plasma is slightly oversaturated, but the in-situ response is subject to other factors. DT and DD also have similar responses with < 2 cm sleeves. This could be because 2 cm is too thin as a moderator for both DT and DD neutrons, and scattered neutrons dominate the detector's response, which is not what we want.

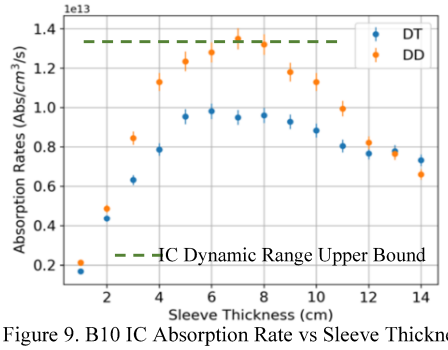

Figure 9. B10 IC Absorption Rate vs Sleeve Thickness.

Neutron flux spectra of selected sleeve thicknesses are in Figure 10. Neutron spectra outside the sleeves while inside the housings, representing pre-moderated fluxes, and those inside the detectors' active volumes, representing moderated fluxes, are compared to examine the moderation performance of the sleeves.

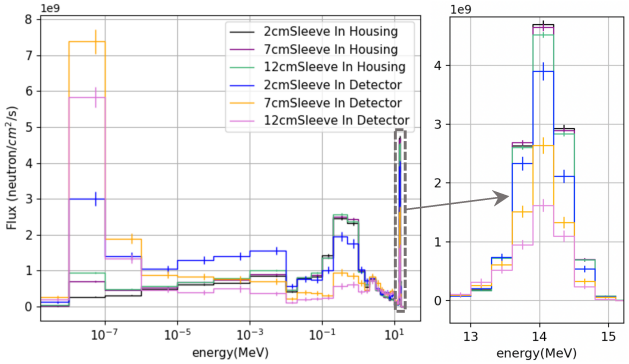

Figure 10. Neutron Spectra Inside the ICs and Housings. "In Housing" Refers to Flux Outside the Sleeves while Inside the Housings; "In Detector" Refers to the Fluxes in the ICs' Active Volumes (the Innermost Green Cylinder in Figure 5b). The source is 5E19 n/s DT Neutrons.

As shown in Figure 10, it's clear that there are more thermal neutrons and fewer fast neutrons after moderation. For the 2 cm sleeve, the 14 MeV peak only drops by about 20%, which confirmed that the 2 cm sleeve does not moderate direct neutrons well. The 12 cm sleeve moderates neutrons the best as it has the lowest 14 MeV peak inside, but the thermal flux inside is lower than the 7 cm sleeve because of block effects.

Quantitatively, according to Table 1, there are only a few percent of < 1 eV neutrons before moderation, and this ratio increases to >33% after moderation by the 7 cm and 12 cm sleeves, but only 14% if by the 2 cm sleeve. As a result, the final decision will be between 6 cm and 14 cm depending on the in-situ signal strength and engineering limitations such as volumes and weights.

Table 1. Fast and Thermal Flux in Housings and Detectors (n/cm²/s)

Sleeve	Energy	In Housing	In Detector
2 cm	Total	8.90E10±5.21E8	9.78E10±1.56E9
	< 1 eV	1.82E9±5.05E7	1.36E10±6.97E8
	> 1 MeV	5.40E10±4.24E8	4.79E10±9.81E8
7 cm	Total	2.94E10±1.38E8	2.87E10±5.62E8
	< 1 eV	1.21E9±2.23E7	9.54E9±3.70E8
	> 1 MeV	1.69E10±1.08E8	1.29E10±3.32E8
12 cm	Total	2.96E10±1.14E8	2.14E10±4.86E8
	< 1 eV	1.49E9±2.21E7	7.35E9±3.11E8
	> 1 MeV	1.65E10±8.75E7	1.04E10±3.08E8

4. *Branching Ratio*

The use of current-mode B10 detectors assumes the 6:94 branching ratio[11] of $^{10}B(n,\alpha_0)$ and $^{10}B(n,\alpha_1)$, whose energy of product ions are 2.79 MeV and 2.31 MeV, respectively. However, according to Figure 8 in Ref. 11, this ratio is only valid for incident neutrons < 100-200 keV. For the current mode of ICs, signal strength is related to the product ions' energies. This might be an issue for B10 ICs' performance in a fast neutron environment.

To evaluate this concern, energy-wise absorption rates of the B10 ICs with 7 cm and 12 cm HDPE sleeves are tallied and plotted in Figure 11. The results confirmed that, in the SPARC environment, more than 99% of the absorptions are induced by neutrons < 100 keV, which suggests that the energy dependence of the branching ratio will not affect the performance of B10 NFMs.

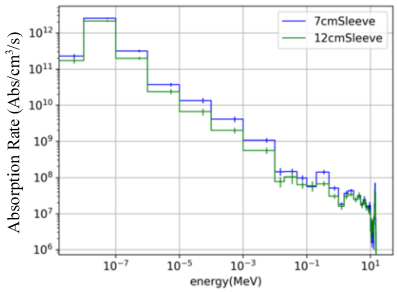

Figure 11. B10 IC Energy-wise Neutron Absorption Rate. Source Rate = 5E19 n/s.

C. U238 Fission Chamber

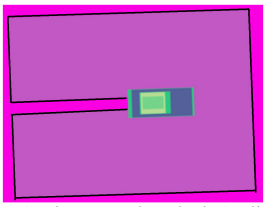

Figure 12. U238 FC Diagram. The Black Outline is the Sleeve.

The proposed U238 FC is a multilayer parallel plate FC operated in counter mode similar to the ones planned for use in ITER's radial neutron camera[12]. Compared to B10, U238 is insensitive to thermal neutrons and thus intrinsically prioritizes direct neutrons. A B-HDPE sleeve is added to prioritize fast neutrons further, as shown in Figure 12. The

30-cm long front opening channel facing towards the 0-degree port provides a collimated line of sight to the plasma.

An OpenMC simulation of U238 FC is verified with the ToFu[13] code. ToFu calculates flux at a given location contributed by sources that can be seen "optically" at the location. ToFu results are analogous to uncollided neutron flux despite some underestimation because ToFu does not count the neutrons penetrating through objects. Uncollided neutron flux at the end of the 30-cm long opening channel, i.e. in front of the detector unit, is tallied by OpenMC and compared with ToFu. OpenMC and ToFu results agree well, as shown in Table 2. OpenMC underestimates the flux compared to ToFu instead of overestimating mainly because OpenMC takes the attenuation in the air into account. The attenuation of 14.1 MeV neutrons in the air could be approximately 10% through 10 meters.

Table 2. Neutron Flux in U238 FC Sleeve Channel. Source Rate=5E19 n/s.

OpenMC (Uncollided)	3.25E10 ± 1.17E9
ToFu (Optical)	3.57E10

OpenMC simulation results are shown in Table 3. Thanks to the intrinsic form factor of U238 FCs and the sleeve, about 60% of the signals, i.e. fission reactions, are induced by direct neutrons. The FOV by the opening channel already covers the entire opening port. The direct/total ratio could be further improved by using a longer channel, which leads to a smaller FOV. Moreover, the 20 cm-thick sleeve and the 10 cm-thick one produce similar results within statistical errors, which means 10 cm is thick enough to shield out scattered neutrons from the side.

Table 3. Fission Rate in U238 FC. Source Rate = 5E19 n/s.

Sleeve Thickness (cm)	10	20
Total fission rate (#/cm^3/s)	6.10E8 ± 2.26E7	5.96E8 ± 2.21E7
Direct fission rate (#/cm^3/s)	3.54E8 ± 1.77E7	3.64E8 ± 1.82E7
Direct/Total ratio	58% ± 3.6%	61% ± 3.8%

IV. CONCLUSIONS and FUTURE WORK

In this work, we explored B10 gamma-compensated ICs and parallel-plate U238 FCs as NFMs for SPARC operation ranges. They are all proposed to be installed by the tokamak hall wall facing the opening 0-degree port on SPARC. A CSG-based OpenMC model has been used for the analysis.

The B10 ICs will have HDPE sleeves, B-HDPE housings, and B-Al covers. B-HDPE and B-Al combined effectively reduce scattered thermal neutrons and make >50% of neutrons around the ICs fast neutrons (> 1 MeV). The HDPE sleeves create more thermal neutrons locally to improve detector responses. 7 cm thickness creates the strongest signal, and 12 cm gives flat responses to DT and DD plasma. In addition, >99% of the absorption reactions are induced by neutrons < 100 keV in SPARC, which eliminates the concern of B10 absorption branching ratio.

The multilayer parallel plate U238 FCs, intrinsically insensitive to thermal neutrons, are equipped with thick B-HDPE sleeves with a 30-cm long opening channel facing the opening port to prioritize direct neutrons. As a result, 60% of the detector responses are induced by direct neutrons.

Next, we will test a U238 FC prototype in the laboratory, including its gamma sensitivity and pulse shape discrimination capability. Also, more NFMs will be explored, including a Li-based scintillator to complement B10 ICs and U238 FCs and calibration range NFMs such as Helium-3 and B10 proportional counters.

V. ACKNOWLEDGEMENTS

This work is supported by Commonwealth Fusion Systems. The authors thank the broader SPARC team.

VI. CONFLICT of INTEREST STATEMENT

All authors are financially supported by CFS either as employees or through sponsored research contracts. CFS is seeking to commercialize fusion energy and may benefit financially from the subject discussed in this manuscript.

VII. BIBLIOGRAPHY

[1] P. Romano, N. Horelik, B. Herman, A. Nelson, B. Forget and K. Smith, "OpenMC: A state-of-the-art Monte Carlo code for research and development," *Annals of Nuclear Energy,* vol. 82, pp. 90-97, 2015.

[2] A. J. Creely et al., "Overview of the SPARC tokamak," *Journal of Plasma Physics,* vol. 86, no. 5, 2020.

[3] P. Raj et al., "Overview of the preliminary design of SPARC's Neutron Diagnostic Systems," in *25th Topical Conference on High Temperature Plasma Diagnostics*, Asheville, NC, 2024.

[4] J. Breslau et al., "TRANSP," Princeton Plasma Physics Lab. (PPPL), Princeton, NJ.

[5] P. Rodriguez-Fernandez et al., "Predictions of core plasma performance for the SPARC tokamak," *Journal of Plasma Physics,* vol. 86, no. 5, 2020.

[6] H.-S. Bosch and G. Hale, "Improved formulas for fusion cross-sections and thermal reactivities," *Nuclear Fusion,* vol. 32, no. 611, 1992.

[7] C. J. Werner, et al., "MCNP6.2 Release Notes, report LA-UR-18-20808," Los Alamos National Laboratory, 2018.

[8] J. Ball et al., "Design of a Spectrometric Detector Unit for the SPARC Neutron Camera," in *25th Topical Conference on High Temperature Plasma Diagnostics*, Asheville, NC, 2024.

[9] S. Mackie et al., "Ion Optical Design of NSPC, the Magnetic Proton Recoil Neutron Spectrometer for Burning Plasma Diagnosis of the SPARC Tokamak," in *25th Topical Conference on High Temperature Plasma Diagnostics*, Asheville, NC, 2024.

[10] D.A.Brown et al., "ENDF/B-VIII," *Nucl. Data Sheets,* vol. 148, no. 1, 2018.

[11] F.-J. Hambsch and H. Bax, "The Standard Branching Ratio 10B(n, alpha0) to 10B(n, alpha1)," *Journal of Nuclear Science and Technology,* vol. Supplement 2, pp. 1402-1405, 2002.

[12] B. Esposito et al., "Progress of Design and Development for the ITER Radial Neutron Camera," *Journal of Fusion Energy,* vol. 41, no. 22, 2022.

[13] D. Vezinet, L. S. Mendoza, F. L. Bourdais, J. Morales and A. Khandelwal, "ToFu Project Github," [Online]. Available: https://tofuproject.github.io/tofu/index.html.